

Impact of nuclear β -decay rates on the r -process rare-earth peak abundancesY.-W. Hao ^{1,2} Y.-F. Niu ^{1,2,*} and Z.-M. Niu ³¹*MOE Frontiers Science Center for Rare Isotopes, Lanzhou University, Lanzhou 730000, People's Republic of China*²*School of Nuclear Science and Technology, Lanzhou University, Lanzhou 730000, People's Republic of China*³*School of Physics and Optoelectronic Engineering, Anhui University, Hefei 230601, People's Republic of China*

(Received 3 August 2023; accepted 17 November 2023; published 19 December 2023)

The impact of β -decay rates of an individual nucleus on the r -process rare-earth peak abundances has been studied in different astrophysical scenarios. The variation in β -decay rates by a factor of 10 can produce large abundance uncertainties in the rare-earth mass region, while fission deposition can significantly reduce this uncertainty, which is not a suggested case by the current simulations of neutron-star mergers with moderately neutron-rich conditions where fission is less active. The most impactful nuclei include even-neutron-number (N) nuclei on the early r -process equilibrium path or r -process freeze-out path and nuclei with $N = 100, 102$, and 104. It is found that the variations in the β -decay rate of nuclei located to the left and right sides of the r -process freeze-out path have significant different effects on rare-earth peak abundance.

DOI: [10.1103/PhysRevC.108.L062802](https://doi.org/10.1103/PhysRevC.108.L062802)

Introduction. The rapid neutron capture process (r -process) of stellar nucleosynthesis is believed to be responsible for the origin of about half of the elements heavier than iron in the universe [1]. The astrophysical sites for r -process nucleosynthesis are still one of the most intriguing open problems. Many candidate sites have been proposed including promising environments in supernovae and neutron star mergers [2,3]. Recent evidence, including the discovery of gravitational waves from the GW170817 and its associated kilonova and GRB 170817A [4,5], indicate neutron-star mergers as one site of the r -process. However, the dominant astrophysical site contributing the production of r -process elements have not yet been unambiguously identified.

The two most prominent features of the r -process abundance in the solar system are the peaks at $A = 130$ and $A = 195$, which are attributed to closed neutron shells occurring at $N = 82$ and $N = 126$ [1,6]. In contrast to the two main peaks, another important feature is the rare-earth peak at $A \approx 165$, lying away from closed neutron shells, and the peak production mechanism is still a controversial topic. Fission cycling has been suggested as a mechanism for obtaining the rare-earth peak, but it depends on the details of the fission fragment distributions, which are not very well understood [7,8]. A dynamical formation mechanism also has been proposed to explain the production of the rare-earth peak, which requires the r -process path encounters the special structure in masses (as well as β -decay and neutron capture rates) in rare-earth mass region during the decay back to stability [9,10]. So the rare-earth peak may contain a unique signature of the late r -process conditions to which the main r -process peaks may be insensitive, and can be used to constrain astrophysical conditions when comparing simulations to the solar r -process abundances [11]. In fact, the rare-earth peak is extremely

sensitive not only to late-time thermodynamic behavior of the astrophysical environment but also to nuclear physics inputs [9–14]. The β -decay rates are important nuclear ingredients that determine the speed of the r -process evolution and the relative abundances in each isotopic chain. The β decay also contributes to shaping the details of the final abundance pattern during the decay back to stability, and β -delayed neutron emission serves as an important source of neutrons for late-time neutron captures [2,3,15].

However, the discrepancies of β -decay half-lives between theory and experiment can be an order of magnitude or more, and the abundance variances produced by such uncertainties of β -decay half-lives in r -process simulations are too large to distinguish the abundance patterns produced by different astrophysical environments [15,16]. Thus, the reductions of uncertainties of β -decay half-lives are necessary. Since it is difficult to measure experimentally the properties of the short-lived nuclei far from stability that participate in the r -process, sensitivity studies to identify the key nuclei that have a substantial impact on the r -process abundances are very important for both future experiments and theoretical studies [15,17,18]. So far, early sensitivity studies [15,19–21] usually focus more on global effects on the abundance distributions caused by β -decay rates variations, and the β -decay rates which are important for the rare-earth peak formation are still not clear. Recently, Kiss *et al.* [13] measured the β -decay properties of neutron-rich exotic Pm, Sm, Eu, and Gd isotopes to constrain the nucleosynthesis yields in the rare-earth region, and the impact of the variation of the half-life of ^{168}Sm on the abundance flow in the nucleosynthesis process is analyzed. However, the systematic analysis about how the variations of the β -decay rates can affect the final rare-earth peak abundance pattern are still rare in the market.

Therefore, in this Letter we perform sensitivity studies focusing on the rare-earth peak formation by varying β -decay rate of each nucleus in the region of interest for the peak

* niuyf@lzu.edu.cn

formation proposed in Ref. [10]. We aim to identify the most influential nuclei and in return show their effects on the rare-earth peak abundance pattern, and further explain the reasons for the different effects caused by nuclei with high sensitivity.

Nucleosynthesis calculations. We use the nuclear network NucNet [22] with more than 6000 isotopes up to No to simulate r -process nucleosynthesis. For our r -process calculations, the β -decay rates, α -decay rates, neutron capture rates are taken from JINA REACLIB database [23]. Experimentally determined masses and reaction rates are adopted if available. Fission is included as in Ref. [24].

We perform r -process calculations using a parametrized trajectory as implemented in Refs. [10,11], where the density as a function of time is given by

$$\rho(t) = \rho_1 \exp(-t/\tau) + \rho_2 \left(\frac{\Delta}{\Delta + t} \right)^n, \quad (1)$$

where $\rho_1 + \rho_2$ is the density at time $t = 0$, and Δ is a constant real number. The parameter n controls the type of late-time r -process thermodynamic evolution. For this work, we consider three distinct astrophysical scenarios: (1) a hot wind r -process with entropy $180 k_B$, initial electron fraction $Y_e = 0.3$, timescale $\tau = 25$ ms, and freeze-out power law $n = 2$, (2) a hot wind r -process with entropy $233 k_B$, $Y_e = 0.1$, $\tau = 35$ ms, and $n = 2$, and (3) a cold wind r -process with entropy $125 k_B$, $Y_e = 0.2$, $\tau = 10$ ms, and $n = 6$. The high entropy conditions are possible in neutrino-driven wind environments, however, we employ lower electron fractions than typically found in detailed supernova models [25] without exotic physics, as implemented in [10,11,15,24,26–29]. It should be noted that there are also many other promising r -process sites, such as neutron star mergers, outflows from magnetohydrodynamic (MHD) supernova or collapsars [30–33], however, the minor changes of the astrophysical parameters almost do not impact our conclusions in the following if the region in the nuclear chart that the nuclear flow can reach is similar under these different astrophysical conditions. We start nucleosynthesis calculations at initial temperature $T = 10$ GK, and the subsequent temperature evolution is determined from the density and entropy [34]. We label these three trajectories as trajectories *hot1*, *hot2*, and *cold*, respectively. Fission is negligible in the *hot1* scenario due to fewer neutrons in the environment. In contrast, a large number of fissioning nuclei can be produced in the *hot2* and *cold* scenarios, and plenty of fission fragments are deposited at around $A = 110$ – 170 region based on the GEF (general description of fission observables) model [24,35,36], which will significantly affect the rare-earth peak formation. In order to exclude the direct effect of fission on rare-earth peak formation, we ran an additional set of simulations in the *cold* scenario with a simple symmetric split for the fission product distributions, which ensures that fission fragments mainly fall in the $A \approx 130$ peak region and do not directly influence the rare-earth peak formation. This set of simulations are labeled as trajectory *cold-sym* in the following.

For our sensitivity studies, baseline abundance patterns are generated with fixed nuclear physics inputs under different astrophysical scenarios. The β -decay rate for a certain nucleus

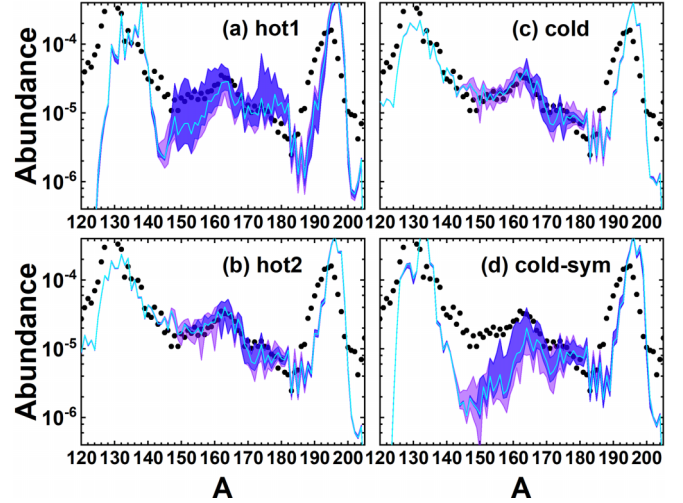


FIG. 1. Uncertainties in final abundances (shaded bands) corresponding to the sensitivity studies for increases and decreases in the β -decay rate by a factor of 10 for each nucleus in the r -process network for different scenarios. Darker shaded bands indicate the uncertainty in final abundances caused by changes in the β -decay rate of the ten nuclei with the highest sensitivity measure F . The cyan lines represent the baseline abundances, and the dots represent the solar r -process abundance pattern [40].

is varied in subsequent simulations. Since the discrepancies between theory and experiment can be one order of magnitude or more, we choose a factor of 10 for our rate variations as in Refs. [15,20,21,28]. We compare the final abundance patterns produced with the β -decay rate variations to the baseline pattern using a sensitivity measure F , which is defined as

$$F = 100 \sum_{A=150}^{178} \frac{|Y_{\beta \times 10}(A) - Y_{\text{ori.}}(A)| + |Y_{\beta / 10}(A) - Y_{\text{ori.}}(A)|}{Y_{\text{ori.}}(A)}, \quad (2)$$

where $Y_{\text{ori.}}(A)$ is the final baseline abundance, and $Y_{\beta \times 10}(A)$ and $Y_{\beta / 10}(A)$ are final abundances of the simulations where β -decay rate is increased or decreased by a factor of 10, respectively.

Results and discussions. The sensitivity studies can be used to estimate the resulting error bars on the abundance pattern due to the uncertainties in β -decay rates as shown in Fig. 1. In each astrophysical scenario, the sensitivity studies are carried out by increasing and decreasing individual β -decay rates by a factor of 10 for 414 nuclei in the r -process simulations, and the resultant 828 r -process abundance patterns form a band, which is represented by the lighter shaded area. The darker shaded bands indicate the uncertainties in final abundances caused by the ten most influential nuclei, which could already cover most of the uncertainties. We find that in *hot1* and *cold-sym* scenarios, such variations in β -decay rates can produce significant effects on the abundance distribution, where the variation of the final abundances could reach up to a factor of 6 in the rare-earth mass region. While in *hot2* and *cold* scenarios, a large number of fission fragments are deposited at the rare-earth peak region, and the width of the uncertainty band is reduced significantly due to the contribution of fis-

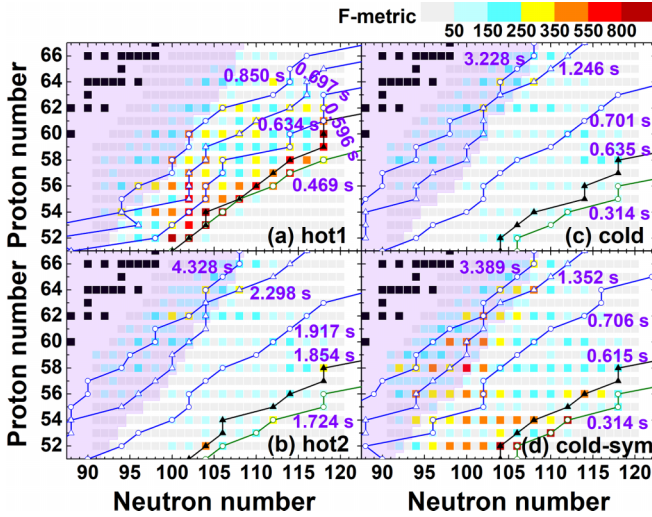


FIG. 2. Sensitivity measures F for β -decay sensitivity studies in four different scenarios. The region of measured β -decay rates from NUBASE 2020 [41] is overlaid with pink color and black squares are stable isotopes. The colored lines represent the r -process paths at different times, with the black line representing paths at the time of r -process freeze-out (defined as the neutron-to-seed ratio $R = 1$), the olive line representing the early r -process paths before freeze-out, and the blue line nearest to the stable nuclei corresponding to the time when the rare-earth peak formation is completed with the timescale of neutron capture being approximately 2 to 3 times of the timescale of β decay.

sion fragments. It also should be noticed that the abundance uncertainty is caused by the variation of only a single nucleus in each r -process simulation, which is different from the conventional uncertainty estimation by global changes of the β -decay rates with different nuclear model or the Monte Carlo variations of nuclear properties as in Refs. [14,15,37], and hence the uncertainty obtained here is much smaller

than that in Refs. [14,15,37]. Clearly, fission deposition can significantly reduce the uncertainties in the final abundance pattern produced due to the uncertainties in β -decay rates. However, the current simulations of neutron-star mergers suggest that the astrophysical conditions for the r -process are moderately neutron-rich [38,39], meaning that the role of fission may be much smaller than previously expected. And in the astrophysical scenarios where fission is not active or the used fission fragment distribution model is unfavorable, the abundance uncertainty caused by β -decay rate variation is too large for precise abundance pattern predictions as shown in Fig. 1.

Figure 2 shows the results of the sensitivity studies for the *hot1*, *hot2*, *cold*, and *cold-sym* scenarios. The most impactful nuclei are listed in Table I, some of which are within current or near future experimental reach, such as ^{162}Ce , ^{159}La , ^{156}Ba , ^{158}Ba , ^{152}Xe . Besides, some nuclei that are not listed in Table I but still have moderate sensitivity, such as ^{168}Sm , ^{170}Sm , ^{164}Nd , ^{166}Nd , ^{160}Ce , are also recommended to be the targets of follow-up experimental researches. As expected, the nuclei with high sensitivity measures F are mainly distributed along the equilibrium r -process path. In the astrophysical scenarios considered here, an equilibrium between neutron capture and photodissociation is also established even in the *cold* and *cold-sym* scenarios. In the $(n, \gamma) \rightleftharpoons (\gamma, n)$ equilibrium phase, the abundances along an isotopic chain are determined by a Saha equation that depends primarily on neutron separation energies and nuclear partition functions. However, the relative abundances of the different isotopic chains are set by the β -decay lifetimes of the most populated nuclei along each chain. In the *hot1* scenarios, the r -process path at freeze-out (defined as the neutron-to-seed ratio $R = 1$) and the early r -process path before freeze-out overlap to some extent, and the equilibrium phases are still maintained at the time of r -process freeze-out, so the final abundances are expected to be sensitive to the change of β -decay rates of the nuclei lying

TABLE I. The most important nuclei with $F > 350$ for the *hot1* scenario and $F > 200$ for *hot2* and *cold* scenarios. Asterisk denotes nucleus with experimental β -decay half-life in NUBASE 2020 [41], and for other nuclei the theoretical half-lives from [50] are also given. Since the solar rare-earth peak cannot be reproduced well in *cold-sym* scenario, the corresponding sensitivity results are not shown here.

Hot1				Hot2				Cold			
Z	A	F	T_β (s)	Z	A	F	T_β (s)	Z	A	F	T_β (s)
52	154	2750.56	0.0076	55	159	539.46	0.0137	52	156	484.28	0.0052
53	157	2199.09	0.0057	61	179	536.30	0.0091	58	176	332.86	0.0040
54	158	1813.12	0.0103	56	164	529.25	0.0096	62	164	308.48	1.4300*
60	178	1719.49	0.0084	55	161	526.08	0.0092	64	168	305.37	3.0300*
52	152	1008.91	0.0097	56	156	501.26	0.0511	54	166	262.09	0.0030
54	160	844.42	0.0073	56	168	491.16	0.0059	64	172	258.73	0.3534
59	177	790.59	0.0053	57	169	446.63	0.0076	62	162	252.62	2.7000*
56	166	724.52	0.0075	58	174	435.65	0.0049	58	174	236.62	0.0049
58	172	716.99	0.0087	58	158	408.40	0.0990*	64	170	233.36	0.4200*
53	155	663.30	0.0099	60	162	393.11	0.3100*	58	172	228.11	0.0087
55	157	637.53	0.0215	54	152	388.89	0.0307	62	166	226.52	0.8000*
56	158	604.20	0.0333	58	162	384.24	0.0466	66	174	221.92	1.7264
54	156	594.81	0.0138	56	160	361.52	0.0199	56	170	211.96	0.0043
55	163	585.89	0.0063	54	154	359.15	0.0211	60	156	211.60	5.0600*
57	171	564.75	0.0056	57	159	356.70	0.0295	62	160	208.57	9.6000*

along these two paths. We find that the rare-earth peak is completely formed at the point where the timescale of neutron capture is approximately 2 to 3 times of the timescale of β decay in the scenarios considered here. It is noted that in the region between r -process paths at freeze-out and at the point of $\tau_{n\gamma} \approx 2\tau_\beta - 3\tau_\beta$, the nuclei with $N = 100, 102$, and 104 have relatively higher F value, which may be related to the rare-earth peak formation mechanism, as mentioned in Refs. [26,27,42–44]. They use Monte Carlo studies of nuclear masses to investigate the trends in the nuclear structure that are necessary to reproduce the observed rare-earth peak abundances, and the results show that the masses with $N = 100, 102$, and particularly $N = 104$, are most important for rare-earth peak formation. Our sensitivity studies also confirm the importance of nuclear structure at $N = 100, 102$, and 104 . An additional notable feature is that the even- N nuclei far away from stability line have larger F value than odd- N nuclei. The reason is that the sensitivity measures are very roughly proportional to the time-integrated abundance of the nuclei [19,21], and the even- N nuclei along the early r -process path that serve as r -process waiting points have the highest abundances, while the odd- N nuclei are much more likely to be depopulated by neutron capture or photodissociation than by waiting for β decay. However, with the evolution of time, the large odd-even staggering patterns of abundances gradually become smoother during the decay back to stability. The abundance difference between odd- N and even- N nuclei decreases, so the nuclei closer to the stability line provide a closer impact between odd and even neutron numbers.

In the *hot2* and *cold* scenarios, the final abundances are largely set by the fission fragment distributions of neutron-rich nuclei, so the sensitivity of the rare-earth peak abundances to β -decay rate variation is diminished, reflecting the role of fission in the robustness of r -process abundances [45–49]. If we use the simple symmetric fission treatment, as in the *cold-sym* scenario, the sensitivity measure F is increased again because the fission fragments do not directly contribute to the rare-earth mass region. However, the solar rare-earth peak abundance cannot be reproduced well by using the symmetric fission treatment as shown in Fig. 1.

As described above, fission deposition significantly reduces the sensitivity of the rare-earth peak abundances to β -decay rate variation. So we next focus on the sensitivity results in the *hot1* scenario where fission is negligible to investigate how a change in β -decay rate affects the final abundance distribution. The different effects of β -decay rate variation on the final abundances are shown in Fig. 3. Two nuclei with high sensitivity measure F were chosen from the *hot1* sensitivity studies of Fig. 2. It is noticed that the increase in β -decay rate of a certain nucleus tends to have smaller effects than the decrease does, because the effects caused by rate increase are limited by the amount of material flowing into this nucleus, so we only focus on the effects caused by rate decrease in the following.

As the β -decay rate of ^{157}I decreases, the abundance increases in the range of more than ten mass numbers near the mass number $A = 157$, which is associated with a decrease of the abundances of nuclei outside the rare-earth peak mass region. While for ^{158}Ba , the abundance increases near

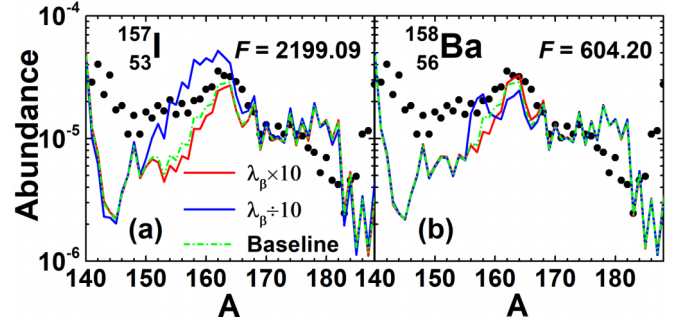


FIG. 3. The effect of β -decay rate on the final rare-earth peak abundances for ^{157}I (a) and ^{158}Ba (b) in the *hot1* scenario. The baseline curve is represented by a dashed green line, and the red and blue lines represent the final abundances corresponding to the ten times and one-tenth of the original β -decay rates of one specific nuclide in the r -process calculations, respectively.

the mass number $A = 158$ but decreases at the higher mass number in the rare-earth peak region, as shown by the blue line in Fig. 3(b). In order to explore systematically these two different effects in the studied nuclei, we use a metric ΔY to classify nuclei with $F > 350$ into two different categories, where ΔY is defined as

$$\Delta Y = \frac{Y_{\beta/10}(A) - Y_{\text{ori.}}(A)}{Y_{\text{ori.}}(A)}. \quad (3)$$

When the β -decay rate of nucleus (Z, A) is reduced by a factor of 10, if abundance variation ΔY at any mass number in the $A - A + 10$ mass range is less than -10% , the nucleus (Z, A) is defined as belonging to Category II, corresponding to a lower abundance at the mass number higher than A , while other nuclei are defined as belonging to Category I, corresponding to an increase in abundance in the range of more than ten mass numbers around mass number A . The results of classification for nuclei with $F > 350$ are shown in Fig. 4. The nuclei in Category I are marked with blue pentagram, while the rest are in Category II. The result shows that the nuclei located

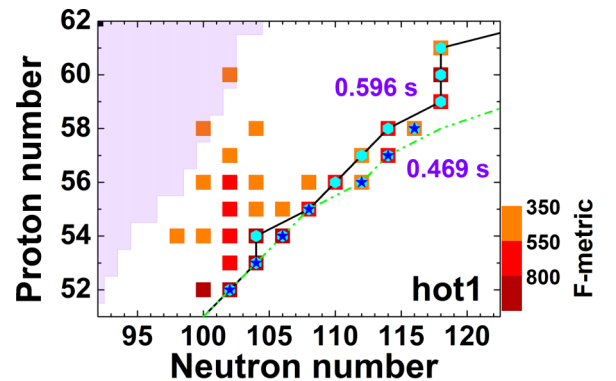


FIG. 4. Categories of nuclei with $F > 350$ with two different effects on abundance distribution caused by β -decay rate variation. The nuclei in Category I are indicated by blue pentagram, while the rest nuclei are in Category II. Nuclei with increase of mass fraction in the rare-earth region ΔX [defined in Eq. (4)] $> 10\%$ are indicated by cyan hexagons. The colored lines represent the r -process paths at different times as in Fig. 2.

both on the freeze-out path and earlier r -process path, as well as those on the right side of the freeze-out path, belong to Category I, while the rest nuclei belong to Category II. This classification is understood as follows. When the β -decay rate of a nucleus decreases and the half-life becomes longer, the abundance of this nucleus will increase in the nucleosynthesis process. We find that if the nuclear flow reaches the nucleus (Z, A) after r -process freeze-out, as the case of ^{158}Ba (belonging to Category II), the longer half-life of the nucleus (Z, A) results in a later population of daughter nuclei on which neutron captures are no longer significantly active due to the low neutron number in the environment at later time. So more material accumulates at the A isobaric mass chain rather than converting into higher masses through neutron capture, resulting in smaller abundances for higher mass numbers, as shown by the blue line in Fig. 3(b). In contrast, if the nuclear flow reaches the nucleus (Z, A) before r -process freeze-out, as the case of ^{157}I (belonging to Category I), the neutron capture of β -decay daughter nuclei does not decrease much when the β -decay rate decreases, and even increases for some nuclei because the number of neutrons in the environment is still very large in this phase, resulting in higher abundances in the range of more than ten mass numbers around A , as shown by the blue line in Fig. 3(a).

In addition, we calculated the total mass fraction in the rare-earth mass region $A = 150\text{--}178$. Nuclei with increase of mass fraction in the rare-earth region $\Delta X > 10\%$ are marked by cyan hexagons in Fig. 4, where ΔX is defined as

$$\Delta X = \sum_{150}^{178} \frac{X_{\beta/10}(A) - X_{\beta \times 10}(A)}{X_{\beta \times 10}(A)}. \quad (4)$$

It is expected that for the nuclei in Category I, as the β -decay rate decreases the total mass fraction in the rare-earth mass region goes up significantly, which means the material accumulated in the rare-earth mass region increases. While for seven nuclei located in the r -process freeze-out path but belonging to Category II, the total mass fraction in the rare-earth mass region still increases by more than 10%, although a decrease in their β -decay rate leads to lower abundances at higher mass numbers. For the nuclei located in the left side of the r -process freeze-out path, the accumulated material in the rare-earth mass region remained almost unchanged as β -decay rate decreases, but the local structure of the rare-earth

peak abundance is changed, that is, the abundance increases at mass number A and decreases at higher mass numbers in the rare-earth mass region. It should be noted that increasing the β -decay rate has the opposite effect of decreasing the rate, but the effect will be much smaller.

Summary. We have performed a sensitivity study of the r -process rare-earth peak abundances to individual β -decay rate in different astrophysical scenarios. We find fission deposition can significantly reduce the uncertainty of the rare-earth peak abundances caused by β -decay rate variation in the astrophysical scenarios where a large number of fission events occur, such as the cases of *hot2* and *cold*. However, it is worth noting that current simulations of neutron-star mergers point towards moderately neutron-rich astrophysical conditions for r -process, suggesting that the role of fission could be considerably smaller than previously expected. Our results show that in moderately neutron-rich astrophysical scenarios, such as *hot1*, the variation of β -decay rates by a factor of 10 introduces large uncertainties in the rare-earth mass region. The most impactful nuclei are those lying along the early r -process equilibrium path or r -process freeze-out path with even neutron number N , especially those with $N = 100, 102$, and 104. When the β -decay rate decreases, for nuclei located in the right side of the r -process freeze-out path, the material accumulated in the rare-earth mass region increases, which results in an increase in abundance in the range of more than ten mass numbers. While for the nuclei located in the left side of the r -process freeze-out path, the accumulated material in the rare-earth mass region remained almost unchanged, but the local structure of the rare-earth peak abundance is changed. It is also noted that nuclei located on the r -process freeze-out path show a combination of both effects. Our work shows clearly the different impact on the rare-earth peak of β -decay half-life of each nucleus in the rare-earth region, which provides a road map for future experimental and theoretical study on β decay and rare-earth peak formation.

Acknowledgments. We acknowledge helpful discussions with Dr. F. Q. Chen and W. L. Lv. This work was supported by the ‘‘Young Scientist Scheme’’ of National Key Research and Development (R&D) Program under Grant No. 2021YFA1601500, the National Natural Science Foundation of China under Grants No. 12075104, No. 11875070, and No. 11935001, and the Anhui project (Z010118169).

-
- [1] E. M. Burbidge, G. R. Burbidge, W. A. Fowler, and F. Hoyle, Synthesis of the elements in stars, *Rev. Mod. Phys.* **29**, 547 (1957).
- [2] T. Kajino, W. Aoki, A. Balantekin, R. Diehl, M. Famiano, and G. Mathews, Current status of r -process nucleosynthesis, *Prog. Part. Nucl. Phys.* **107**, 109 (2019).
- [3] J. J. Cowan, C. Sneden, J. E. Lawler, A. Aprahamian, M. Wiescher, K. Langanke, G. Martínez-Pinedo, and F.-K. Thielemann, Origin of the heaviest elements: The rapid neutron-capture process, *Rev. Mod. Phys.* **93**, 015002 (2021).
- [4] B. P. Abbott, R. Abbott, T. D. Abbott, F. Acernese, K. Ackley, C. Adams, T. Adams, P. Addesso, R. X. Adhikari, V. B. Adya, C. Affeldt, and M. Afrough, Gw170817: Observation of gravitational waves from a binary neutron star inspiral, *Phys. Rev. Lett.* **119**, 161101 (2017).
- [5] B. P. Abbott, R. Abbott, T. D. Abbott, F. Acernese, K. Ackley, C. Adams, T. Adams, P. Addesso, R. X. Adhikari, V. B. Adya, C. Affeldt, M. Afrough, B. Agarwal, M. Agathos, K. Agatsuma, N. Aggarwal, O. D. Aguiar, L. Aiello, A. Ain, P. Ajith *et al.*, Gravitational waves and gamma-rays from a binary neutron star merger: GW170817 and GRB 170817A, *Astrophys. J. Lett.* **848**, L13 (2017).
- [6] A. Arcones and G. F. Bertsch, Nuclear correlations and the r process, *Phys. Rev. Lett.* **108**, 151101 (2012).
- [7] D. N. Schramm and W. A. Fowler, Synthesis of superheavy elements in the r -process, *Nature (London)* **231**, 103 (1971).

- [8] S. Goriely, J.-L. Sida, J.-F. Lemaître, S. Panebianco, N. Dubray, S. Hilaire, A. Bauswein, and H.-T. Janka, New fission fragment distributions and r -process origin of the rare-earth elements, *Phys. Rev. Lett.* **111**, 242502 (2013).
- [9] R. Surman, J. Engel, J. R. Bennett, and B. S. Meyer, Source of the rare-earth element peak in r -process nucleosynthesis, *Phys. Rev. Lett.* **79**, 1809 (1997).
- [10] M. R. Mumpower, G. C. McLaughlin, and R. Surman, Formation of the rare-earth peak: Gaining insight into late-time r -process dynamics, *Phys. Rev. C* **85**, 045801 (2012).
- [11] M. R. Mumpower, G. C. McLaughlin, and R. Surman, The rare earth peak: An overlooked r -process diagnostic, *Astrophys. J.* **752**, 117 (2012).
- [12] A. Arcones and G. Martínez-Pinedo, Dynamical r -process studies within the neutrino-driven wind scenario and its sensitivity to the nuclear physics input, *Phys. Rev. C* **83**, 045809 (2011).
- [13] G. G. Kiss, A. Vitez-Sveicz, Y. Saito, A. Tarifeno-Saldivia, M. Pallas, J. L. Tain, I. Dillmann, J. Agramunt, A. Algora, C. Domingo-Pardo, A. Estrade, C. Appleton, J. M. Allmond, and P. Aguilera, Measuring the beta-decay properties of neutron-rich exotic Pm, Sm, Eu, and Gd isotopes to constrain the nucleosynthesis yields in the rare-earth region, *Astrophys. J.* **936**, 107 (2022).
- [14] J. Chen, J. Y. Fang, Y. W. Hao, Z. M. Niu, and Y. F. Niu, Impact of nuclear β -decay half-life uncertainties on the r -process simulations, *Astrophys. J.* **943**, 102 (2023).
- [15] M. Mumpower, R. Surman, G. McLaughlin, and A. Aprahamian, The impact of individual nuclear properties on r -process nucleosynthesis, *Prog. Part. Nucl. Phys.* **86**, 86 (2016).
- [16] Z. Li, Z. M. Niu, and B. H. Sun, Influence of nuclear physics inputs and astrophysical conditions on r -process, *Sci. China: Phys., Mech. Astron.* **62**, 982011 (2019).
- [17] M. Mumpower, R. Surman, D. L. Fang, M. Beard, and A. Aprahamian, The impact of uncertain nuclear masses near closed shells on the r -process abundance pattern, *J. Phys. G: Nucl. Part. Phys.* **42**, 034027 (2015).
- [18] M. R. Mumpower, R. Surman, D.-L. Fang, M. Beard, P. Möller, T. Kawano, and A. Aprahamian, Impact of individual nuclear masses on r -process abundances, *Phys. Rev. C* **92**, 035807 (2015).
- [19] J. Cass, G. Passucci, R. Surman, and A. Aprahamian, Beta decay and the r -process, *Proceedings of Science (NIC XII)*, 154(2012).
- [20] R. Surman, M. Mumpower, J. Cass, I. Bentley, A. Aprahamian, and G. C. McLaughlin, Sensitivity studies for r -process nucleosynthesis in three astrophysical scenarios, *EPJ Web Conf.* **66**, 07024 (2014).
- [21] M. Mumpower, J. Cass, G. Passucci, R. Surman, and A. Aprahamian, Sensitivity studies for the main r process: β -decay rates, *AIP Adv.* **4**, 041009 (2014).
- [22] <http://sourceforge.net/p/nucnet-tools>.
- [23] <https://jinaweb.org/reactlib/db>.
- [24] Y. W. Hao, Y. F. Niu, and Z. M. Niu, Influence of spontaneous fission rates on the r -process nucleosynthesis, *Astrophys. J.* **933**, 3 (2022).
- [25] G. Martínez-Pinedo, T. Fischer, and L. Huther, Supernova neutrinos and nucleosynthesis, *J. Phys. G: Nucl. Part. Phys.* **41**, 044008 (2014).
- [26] M. R. Mumpower, G. C. McLaughlin, R. Surman, and A. W. Steiner, The link between rare-earth peak formation and the astrophysical site of the r process, *Astrophys. J.* **833**, 282 (2016).
- [27] M. R. Mumpower, G. C. McLaughlin, R. Surman, and A. W. Steiner, Reverse engineering nuclear properties from rare earth abundances in the r process, *J. Phys. G: Nucl. Part. Phys.* **44**, 034003 (2017).
- [28] J. Wu, S. Nishimura, G. Lorusso, P. Möller, E. Ideguchi, P.-H. Regan, G. S. Simpson, P.-A. Söderström, P. M. Walker, H. Watanabe, Z. Y. Xu, H. Baba, F. Browne, R. Daido, P. Doornenbal, Y. F. Fang, N. Fukuda, G. Gey, T. Isobe, Z. Korkulu *et al.*, 94β -decay half-lives of neutron-rich ^{55}Cs to ^{67}Ho : Experimental feedback and evaluation of the r -process rare-earth peak formation, *Phys. Rev. Lett.* **118**, 072701 (2017).
- [29] Y. Hao, Y. Niu, and Z. Niu, Sensitivity of the r -process rare-earth peak abundances to nuclear masses, *Phys. Lett. B* **844**, 138092 (2023).
- [30] Y. Yamazaki, Z. He, T. Kajino, G. Mathews, M. Famiano, X. Tang, and J. Shi, Possibility to identify the contributions from collapsars, supernovae, and neutron star mergers from the evolution of the r -process mass abundance distribution, *Astrophys. J.* **933**, 112 (2022).
- [31] C. Winteler, R. Käppeli, A. Perego, A. Arcones, N. Vasset, N. Nishimura, M. Liebendörfer, and F. K. Thielemann, Magnetorotationally driven supernovae as the origin of early galaxy r -process elements, *Astrophys. J. Lett.* **750**, L22 (2012).
- [32] K. Hotokezaka, P. Beniamini, and T. Piran, Neutron star mergers as sites of r -process nucleosynthesis and short gamma-ray bursts, *Int. J. Mod. Phys. D* **27**, 1842005 (2018).
- [33] S. Wanajo, Y. Sekiguchi, N. Nishimura, K. Kiuchi, K. Kyutoku, and M. Shibata, Production of all the r -process nuclides in the dynamical ejecta of neutron star mergers, *Astrophys. J. Lett.* **789**, L39 (2014).
- [34] B. S. Meyer, r -process nucleosynthesis without excess neutrons, *Phys. Rev. Lett.* **89**, 231101 (2002).
- [35] <http://www.cenbg.in2p3.fr/GEF>.
- [36] N. Vassh, R. Vogt, R. Surman, J. Randrup, T. M. Sprouse, M. R. Mumpower, P. Jaffke, D. Shaw, E. M. Holmbeck, Y. Zhu, and G. C. McLaughlin, Using excitation-energy dependent fission yields to identify key fissioning nuclei in r -process nucleosynthesis, *J. Phys. G: Nucl. Part. Phys.* **46**, 065202 (2019).
- [37] I. V. Panov, Beta-decay rate as an important factor of production of heavy nuclei in the r -process, *Phys. Part. Nucl.* **54**, 660 (2023).
- [38] S. Fahlman and R. Fernandez, Hypermassive neutron star disk outflows and blue kilonovae, *Astrophys. J. Lett.* **869**, L3 (2018).
- [39] O. Just, V. Vijayan, Z. Xiong, S. Goriely, T. Soultanis, A. Bauswein, J. Guilet, and H.-T. Janka, End-to-end kilonova models of neutron star mergers with delayed black hole formation, *Astrophys. J. Lett.* **951**, L12 (2023).
- [40] C. Sneden, J. J. Cowan, and R. Gallino, Neutron-capture elements in the early galaxy, *Annu. Rev. Astron. Astrophys.* **46**, 241 (2008).
- [41] F. Kondev, M. Wang, W. Huang, S. Naimi, and G. Audi, The NUBASE2020 evaluation of nuclear physics properties, *Chin. Phys. C* **45**, 030001 (2021).
- [42] R. Orford, N. Vassh, J. A. Clark, G. C. McLaughlin, M. R. Mumpower, G. Savard, R. Surman, A. Aprahamian, F.

- Buchinger, M. T. Burkey, D. A. Gorelov, T. Y. Hirsh, J. W. Klimes, G. E. Morgan, A. Nystrom, and K. S. Sharma, Precision mass measurements of neutron-rich neodymium and samarium isotopes and their role in understanding rare-earth peak formation, *Phys. Rev. Lett.* **120**, 262702 (2018).
- [43] R. Orford, N. Vassh, J. A. Clark, G. C. McLaughlin, M. R. Mumpower, D. Ray, G. Savard, R. Surman, F. Buchinger, D. P. Burdette, M. T. Burkey, D. A. Gorelov, J. W. Klimes, W. S. Porter, K. S. Sharma, A. A. Valverde, L. Varriano, and X. L. Yan, Searching for the origin of the rare-earth peak with precision mass measurements across Ce–Eu isotopic chains, *Phys. Rev. C* **105**, L052802 (2022).
- [44] N. Vassh, G. C. McLaughlin, M. R. Mumpower, and R. Surman, Markov chain Monte Carlo predictions of neutron-rich lanthanide properties as a probe of r-process dynamics, *Astrophys. J.* **907**, 98 (2021).
- [45] J. Beun, G. C. McLaughlin, R. Surman, and W. R. Hix, Fission cycling in a supernova r process, *Phys. Rev. C* **77**, 035804 (2008).
- [46] S. Goriely, A. Bauswein, and H.-T. Janka, r -process nucleosynthesis in dynamically ejected matter of neutron star mergers, *Astrophys. J. Lett.* **738**, L32 (2011).
- [47] O. Korobkin, S. Rosswog, A. Arcones, and C. Winteler, On the astrophysical robustness of the neutron star merger r -process, *Mon. Not. R. Astron. Soc.* **426**, 1940 (2012).
- [48] J. d. J. Mendoza-Temis, M.-R. Wu, K. Langanke, G. Martínez-Pinedo, A. Bauswein, and H.-T. Janka, Nuclear robustness of the r process in neutron-star mergers, *Phys. Rev. C* **92**, 055805 (2015).
- [49] J.-F. Lemaître, S. Goriely, A. Bauswein, and H.-T. Janka, Fission fragment distributions and their impact on the r -process nucleosynthesis in neutron star mergers, *Phys. Rev. C* **103**, 025806 (2021).
- [50] P. Möller, M. Mumpower, T. Kawano, and W. Myers, Nuclear properties for astrophysical and radioactive-ion-beam applications (II), *At. Data Nucl. Data Tables* **125**, 1 (2019).